

Non-magnetic ground state of PuO₂

A. B. Shick,¹ J. Kolorenc,¹ L. Havela,² T. Gouder,³ and R. Caciuffo³

¹*Institute of Physics, ASCR, Na Slovance 2, CZ-18221 Prague, Czech Republic*

²*Department of Condensed Matter Physics, Charles University,
Ke Karlovu 5, CZ-12116, Prague, Czech Republic*

³*European Commission, Joint Research Centre, Institute for
Transuranium Elements, Postfach 2340, D-76125 Karlsruhe, Germany*

(Dated: June 15, 2021)

The correlated band theory implemented as a combination of the local density approximation with the exact diagonalization of the Anderson impurity model is applied to PuO₂. We obtain an insulating electronic structure consistent with the experimental photoemission spectra. The calculations yield the band gap of 1.8 eV and a non-magnetic singlet ground state that is characterized by a non-integer filling of the plutonium f shell ($n_f \approx 4.5$). Due to sizeable hybridization of the f shell with the p states of oxygen, the ground state is more complex than the four-electron Russell-Saunders 5I_4 manifold split by the crystal field. The inclusion of hybridization improves the agreement between the theory and experiment for the magnetic susceptibility.

PACS numbers: 71.20,71.27+a,75.40.Cx

In order to fully utilize the potential of nuclear power, maintaining at the minimum level the risks associated with the deployment of this technology, it is necessary to solve the problems of characterization, treatment, and disposal of high-level nuclear waste. On the time scale of several hundred years, the waste from the open fuel cycle will predominantly contain Pu and minor actinides. Their geological disposal requires a waste handling technology of exceptional durability, with highly reduced risk of accidental events. That is why the comprehensive knowledge of the physical and chemical properties of actinide-based oxides (AnO₂, An = Th, U, Np, Pu, Am, Cm), which constitute the main part of the the long-lived nuclear waste, remains a key topic of condensed matter theory.

PuO₂ crystalises in the well-known CaF₂ fluorite structure, with eight-coordinated Pu, and four-coordinated O. For the divalent oxygen, the stoichiometry implies $5f^4$ configuration for Pu⁴⁺. PuO₂ is an insulator with a band gap of 1.8 eV [1] and a temperature independent magnetic susceptibility [2]. Recent nuclear magnetic resonance studies suggest a vanishing local magnetic moment in this compound [3].

Whilst experimentally the absence of magnetism is clear, its theoretical understanding remains controversial. The crystal-field (CF) theory [4] explains this non-magnetic behaviour in terms of a Γ_1 nonmagnetic singlet ground state, which results from the CF splitting of the $J = 4$ (5I_4) manifold. The CF picture is consistent with the inelastic neutron scattering spectra [5] observing a single peak, corresponding to the $\Gamma_1 \rightarrow \Gamma_4$ transition, at the energy of 123 meV. However, the measured value of the magnetic susceptibility $\chi(T)$ is only 50 % of what one would expect from the Van Vleck coupling, and its temperature dependence is weaker than the one predicted by the CF model. The average value of χ in the tempera-

ture interval up to about 1000 K can be reproduced, if the Γ_4 level is taken at 284 meV and not at 123 meV as observed. Several alternative mechanisms that could decrease the magnitude of the susceptibility while keeping the $\Gamma_1 \rightarrow \Gamma_4$ gap at 123 meV have been proposed. One of them is an effective reduction of the orbital moment by Pu $f - O p$ covalency [5], another involves a negative contribution to χ due to antiferromagnetic Weiss exchange field (see e.g. [4] and references therein). Nevertheless, the temperature independence of the susceptibility is not explained in these models.

The band-theoretical modeling of the electronic, structural, and magnetic character of actinide materials and their $5f$ states is very difficult. The conventional density functional theory (DFT) in the local spin density (LSDA) and generalized gradient (GGA) approximations falls short to explain the insulating character of PuO₂ as well as other actinide oxides [6]. It is now widely accepted that in order to successfully model the actinide materials, the electron correlations need to be accounted for beyond the conventional DFT. One of the possibilities is provided by the so-called hybrid exchange-correlation functionals [6]. Unfortunately, these calculations yield the anti-ferromagnetic ground state in disagreement with experiments.

Contrary to the hybrid functionals, the so-called LSDA+Hubbard U (LDA+ U) functional can produce an insulating non-magnetic solution for PuO₂ [7, 8]. However, this solution is not the minimum energy state, and ferromagnetic and anti-ferromagnetic spin-polarized LDA+ U solutions are lower in energy. Thus the Pu atom magnetic moment is not quenched, and the experimentally observed temperature independent magnetic susceptibility of PuO₂ is not explained by LDA+ U calculations.

In this paper, we extend the LDA+ U method making

use of a combination of LDA with the exact diagonalization of the Anderson impurity model (ED) [9, 10]. We show that the LDA+ED calculations with the Coulomb $U = 6.5$ eV and the exchange $J = 0.5$ eV yield a non-magnetic singlet ground state with f -shell occupation $n_f \approx 4.5$ at the Pu atoms. The non-integer filling of the f shell is a consequence of a hybridization with the p states of oxygen. In contrast, the ionic bonding with formally divalent oxygen assumed in the crystal-field theory would require an integer filling ($n_f = 4$). The ground state is found to be separated from the first excited triplet state by 126 meV. The LDA+ED electronic structure is insulating with a band gap of 1.8 eV and the calculated density of states (DOS) is consistent with the experimental results of photoelectron spectroscopy (PES).

The starting point of our approach is the multi-band Hubbard Hamiltonian $H = H^0 + H^{\text{int}}$, where H^0 is the one-particle Hamiltonian found from *ab initio* electronic structure calculations of a periodic crystal; H^{int} is the on-site Coulomb interaction [11] describing the $5f$ -electron correlation. We use the LDA for the electron interactions in other than f shells. The effects of the interaction Hamiltonian H^{int} on the electronic structure are described with the aid of an auxiliary impurity model describing the complete seven-orbital $5f$ shell. This multi-orbital impurity model includes the full spherically symmetric Coulomb interaction, the spin-orbit coupling (SOC), and the crystal field. The corresponding Hamiltonian can be written as [12]

$$\begin{aligned}
H_{\text{imp}} = & \sum_{\substack{kmm' \\ \sigma\sigma'}} [\epsilon^k]_{mm'}^{\sigma\sigma'} b_{km\sigma}^\dagger b_{km'\sigma'} + \sum_{m\sigma} \epsilon_f f_{m\sigma}^\dagger f_{m\sigma} \\
& + \sum_{mm'\sigma\sigma'} [\xi \mathbf{1} \cdot \mathbf{s} + \Delta_{\text{CF}}]_{mm'}^{\sigma\sigma'} f_{m\sigma}^\dagger f_{m'\sigma'} \\
& + \sum_{\substack{kmm' \\ \sigma\sigma'}} \left([V^k]_{mm'}^{\sigma\sigma'} f_{m\sigma}^\dagger b_{km'\sigma'} + \text{h.c.} \right) \\
& + \frac{1}{2} \sum_{\substack{mm'm'' \\ m'''\sigma\sigma'}} U_{mm'm''m'''} f_{m\sigma}^\dagger f_{m'\sigma'}^\dagger f_{m'''\sigma'} f_{m''\sigma},
\end{aligned} \quad (1)$$

where $f_{m\sigma}^\dagger$ creates an electron in the $5f$ shell and $b_{m\sigma}^\dagger$ creates an electron in the “bath” that consists of those host-band states that hybridize with the impurity $5f$ shell. The energy position ϵ_f of the impurity level, and the bath energies ϵ^k are measured from the chemical potential μ . The parameter ξ specifies the strength of the SOC and Δ_{CF} is the crystal-field potential at the impurity. The parameter matrices V^k describe the hybridization between the $5f$ states and the bath orbitals at energy ϵ^k .

The band Lanczos method [9] is employed to find the lowest-lying eigenstates of the many-body Hamiltonian H_{imp} and to calculate the one-particle Green’s function $[G_{\text{imp}}(z)]_{mm'}^{\sigma\sigma'}$ in the subspace of the f orbitals at low temperature ($k_{\text{B}}T = \beta^{-1} = 1/500$ eV). Then, with the aid of

the local Green’s function $G_{\text{imp}}(z)$, we evaluate the occupation matrix $n_{\gamma_1\gamma_2} = \frac{1}{\beta} \sum_{\omega} [G_{\text{imp}}(i\omega)]_{\gamma_1\gamma_2} + \frac{1}{2} \delta_{\gamma_1\gamma_2}$, where the composite index $\gamma \equiv (lm\sigma)$ labels spinorbitals.

The matrix $n_{\gamma_1\gamma_2}$ is used to construct an effective LDA+ U potential V_U , which is inserted into Kohn-Sham-like equations [13]:

$$[-\nabla^2 + V_{\text{LDA}}(\mathbf{r}) + V_U + \xi(\mathbf{1} \cdot \mathbf{s})] \Phi_{\mathbf{k}}^b(\mathbf{r}) = \epsilon_{\mathbf{k}}^b \Phi_{\mathbf{k}}^b(\mathbf{r}). \quad (2)$$

These equations are iteratively solved until self-consistency over the charge density is reached. In each iteration a new value of the $5f$ -shell occupation is obtained from the solution of Eq. (2), and the next iteration is started by solving Eq. (1) for the updated $5f$ -shell filling. The self-consistent procedure was repeated until the convergence of the $5f$ -manifold occupation n_f was better than 0.02.

Once the self-consistency is reached, the eigenvalues $\epsilon_{\mathbf{k}}$ of Eq. (2) are corrected to account for the selfenergy $\Sigma(\epsilon)$ of the impurity model Eq. (1), see supplementary material for additional details. We make use of the first-order perturbation theory to write an eigenvalue correction,

$$\mathbf{E}_{\mathbf{k}}^n = \epsilon_{\mathbf{k}}^n + \text{Re} \langle \Phi_{\mathbf{k}}^n | \Sigma(\epsilon_{\mathbf{k}}^n) - V_U | \Phi_{\mathbf{k}}^n \rangle. \quad (3)$$

The SOC parameters $\xi = 0.30$ eV for PuO₂ was determined from LDA calculations. CF effects were described by the crystal field potential for the cubically coordinated f -shell,

$$\begin{aligned}
\Delta_{\text{CF}} = & \frac{16\sqrt{\pi}}{3} V_4 \left(Y_4^0 + \sqrt{\frac{10}{7}} \text{Re} Y_4^4 \right) \\
& + 32 \sqrt{\frac{\pi}{13}} V_6 (Y_6^0 - \sqrt{14} \text{Re} Y_6^4),
\end{aligned} \quad (4)$$

where V_4 and V_6 were chosen as external parameters. In the actual calculations, we used the values $V_4 = -0.151$ eV and $V_6 = 0.031$ eV deduced from experimental data in Ref. [5], and close to the estimate given in [14]. The CF parameters could be also calculated using *ab-initio* approaches [15], and we plan to do so in the future.

In order to specify the bath parameters, we assume that LDA represents the non-interacting model for PuO₂, and associate with it the solution of Eq. (1) without the last Coulomb-interaction term. Moreover, we assume that the first and fourth terms in Eq. (1) are diagonal in $\{j, j_z\}$ representation. Next, we obtain $V_{k=1}^{j=5/2,7/2}$ and $\epsilon_{k=1}^{5/2,7/2}$ from LDA hybridization function $\Delta(\epsilon) = -\frac{1}{\pi N_f} \text{Im} \text{Tr}[G^{-1}(\epsilon + i\delta)]$ where $N_f = 6$ for $j = 5/2$, $N_f = 8$ for $j = 7/2$, and G is the LDA Green’s function. The hybridization function $\Delta(\epsilon)$ is shown in Fig. 1 together with the O- p and Pu- f -projected LDA densities of states. As follows from Fig. 1, the most essential hybridization occurs in the energy region of the O- p states. We set $\epsilon_{k=1}^{5/2,7/2}$ to the -2.92 eV peak position of $\Delta(\epsilon)$, and obtain $V_{k=1}^{j=5/2} = 1.46$ eV, and $V_{k=1}^{j=7/2} = 1.62$ eV at the peak position of $\Delta(\epsilon)$.

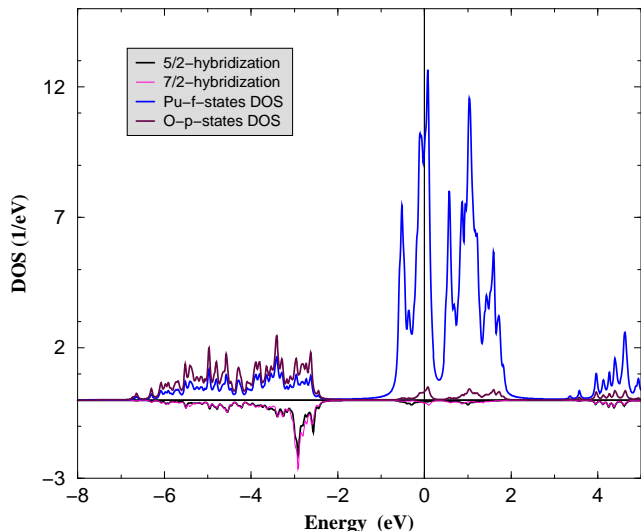


FIG. 1: (Color online) The O- p and Pu- f -projected DOS, and the hybridization function $\Delta(\epsilon)$ (the negative y -axis scale, eV).

The Slater integral F_0 (Coulomb U) is regarded as an adjustable parameter; calculations have been performed for $U = 4.5, 5.5,$ and 6.5 eV, within the range commonly considered in the literature. For the other Slater integrals we have used the values $F_2 = 5.96$ eV, $F_4 = 3.982$ eV, and $F_6 = 2.946$ eV that have been obtained by scaling the atomic Hartree-Fock results [16] to approximately 60% to account for configuration interactions and screening effects. The screened integrals correspond to the Hund's exchange $J = 0.5$ eV, which is in the ballpark of the values used in the LDA+ U [6] and LDA+DMFT [17] calculations. For the double-counting term (included in the potential V_U) we have adopted the fully-localized (or atomic-like) limit (FLL) $V_{dc} = U(n_f - 1/2) - J(n_f - 1)/2$.

In the calculations we used an in-house implementation [18, 19] of the full-potential linearized augmented plane wave (FP-LAPW) method that includes both scalar-relativistic and spin-orbit coupling effects. The calculations were carried out assuming a paramagnetic state, and the cubic fluorite crystal structure. We set the radius of the Pu atomic sphere to 2.65 a.u., and the O atomic sphere to 1.70 a.u. The parameter $R_{\text{Pu}} \times K_{\text{max}} = 9.3$ determined the basis set size, and the Brillouin zone was sampled with 4000 k points.

Now we turn to the results of LDA+ED calculations. For the set of $U = 4.5$ eV and $J = 0.5$ eV, solving self-consistently Eq. (1) and Eq. (2), we obtain the f occupation $n_f = 4.58$ close to conventional LDA+ U with the same U and J ($n_f = 4.56$) as well as to the occupation deduced from the $4f$ X-ray photoemission spectroscopy (XPS, $n_f = 4.65$ [20]). After applying the eigenvalue correction Eq. (3), we do not obtain an insulating state. Once the Coulomb U is increased, say to 5.5 eV,

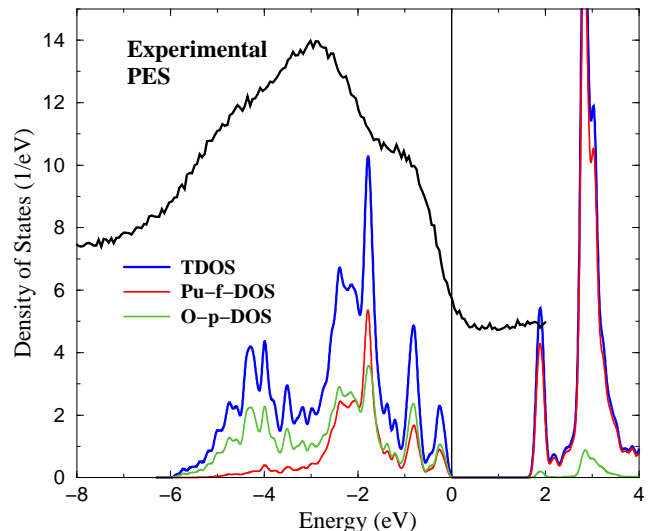


FIG. 2: (Color online) The total, O- p and Pu- f -projected DOS from LDA+ED calculations with $U = 6.5$ eV, $J = 0.5$ eV, together with the experimental PES (spectrum, recorded with the He-II excitation, photon energy 40.81 eV). Note that the PES spectrum is adjusted to match the upper edge with the zero energy.

the PuO₂ becomes an insulator with the band gap of 1.4 eV (see supplementary material, Table S2). For the Coulomb $U = 6.5$ eV (and $J = 0.5$ eV), we obtain an insulating solution with a band gap of 1.8 eV. When the value of $J = 0.6$ eV is used, the band gap value is slightly reduced to 1.6 eV. The corresponding total density of states (TDOS), the Pu atom f -state, and the O atom p -state partial DOS are shown in Fig. S2.

The experimental PES [21–23] (see Fig. S2, note the horizontal shift of the data) is usually obtained on PuO₂ films prepared by reactive sputter deposition from an α -Pu target in an Ar/O₂ plasma. The O₂ partial pressure was adjusted to obtain the correct stoichiometry. Peaks are observed at 2 and 4 eV binding energy (BE), with a shoulder at 6 eV BE. The orbital parentage of the peaks can be deduced by comparing the intensities obtained for He-I and He-II radiation (photon energy equal to 21.22 eV and 40.81 eV, respectively). The He-I spectrum is dominated by the O- p emission, whereas for He-II the Pu- f and O- p contributions are comparable. It is concluded that the 2 eV BE peak stems from the Pu- f states. This peak is usually considered as an indication of the f^4 nominal configuration, corresponding to Pu⁴⁺ oxidation state. The next (4 eV BE) peak is more intense and broad. The He-II and He-I spectral difference indicates a substantial O- p character of this peak. The shoulder at 6 eV BE is associated mostly with the O- p states. As the calculations associate the upper edge of the conduction band with zero binding energy, the experimental spectrum was shifted for the sake of comparison towards the zero energy, as well.

The LDA+ED DOS shown in Fig. S2 has the peak with the mixed Pu- f and O- p characters at ≈ 0.8 eV below the E_F (with additional smaller satellite closer to the E_F). Another broad peak at ≈ -2 eV has more intensity (for both f and p states). And there is a broad, dominantly O- p character, shoulder between -3 and -6 eV. Thus, if we consider the difference in the peaks positions, they correspond reasonably to the experiment. Their absolute values differ from the experimental BE [21–23] by ≈ 1 to 1.5 eV. The reason is that in PES experiments the Fermi level falls in the middle of the band gap, whilst the upper edge of the conduction band defines the Fermi level in the calculations. Both the experiment and calculations suggest a mixture of f^4 and f^5 configurations in the ground state due to Pu-5 f and O-2 p hybridization.

Now we turn to the salient theme of our investigation, the ground state of the impurity model Eq. (1). This ground state is a singlet formed by the 5 f shell and the bath with occupation numbers $\langle n_f \rangle = 4.52$ in the f shell and $\langle n_{bath} \rangle = 13.48$ in the bath states. Since the ground state is a singlet, any magnetic or multipolar degree of freedom is frozen when the temperature is well below the gap between the ground state and excited states. The calculated energy difference between this ground state and the first excited states (triplet) is 126 meV, very close to the experimental value 123 meV, observed in the inelastic neutron scattering spectra [5]. Neither the ground state nor the excited states are exact crystal-field states since they involve the p states of oxygen.

Analogously to the crystal-field theory, the impurity model can be used to estimate the magnetic susceptibility and its temperature dependence by adding the action of an external magnetic field B_z to Eq. (1),

$$\hat{H}_B = - \sum_{m\sigma} \mu_B B_z \left([\hat{l}_z + 2\hat{s}_z]_{mm}^{\sigma\sigma} \hat{f}_{m\sigma}^\dagger \hat{f}_{m\sigma} + [2\hat{s}_z]_{mm}^{\sigma\sigma} \hat{b}_{m\sigma}^\dagger \hat{b}_{m\sigma} \right). \quad (5)$$

The bath originates from the LDA oxygen bands and hence the magnetic field couples only to the spin degrees of freedom in this part of the impurity model. When the magnetic field is weak and the linear-response regime applies we can get the molar magnetic susceptibility from the induced f -shell magnetic moment $m_z(T) = \mu_B \langle \hat{l}_z + 2\hat{s}_z \rangle$ as $\chi_{\text{imp}}(T) = \mu_0 N_A m_z(T) / B_z$, where μ_0 stands for the vacuum permeability.

The susceptibility χ_{imp} calculated for $U = 6.5$ eV and $J = 0.5$ eV is shown in Fig. 3 in comparison with the susceptibility χ_{CF} from the crystal-field theory, that is, from Eq. (1) without the bath. The hybridization of the f orbitals with the ligand states reduces the magnitude of the susceptibility as well as its temperature dependence and hence brings the theory closer to the experimental findings [2]. Here we in fact estimate the magnitude of the covalency effects discussed in [5]. Furthermore, it

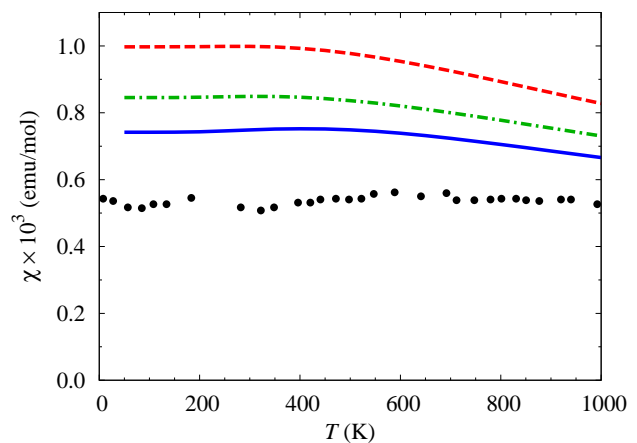


FIG. 3: (Color online) Temperature dependence of the molar magnetic susceptibility calculated in the crystal-field theory (χ_{CF} , red dashed line) and in the impurity model (χ_{imp} , green dot-dashed line) for $U = 6.5$ eV and $J = 0.5$ eV. Blue solid line shows χ_{imp} with the exchange enlarged to $J = 0.6$ eV. Black dots are the experimental data from [2].

turns out that χ_{imp} is sensitive to the exchange parameter J , whereas it is essentially independent on U . With $J = 0.6$ eV, the temperature dependence is further suppressed and the magnitude of χ_{imp} is only about 35% larger than the experiment (see Fig. 3 and compare to nearly 100% overestimation of the crystal field theory alone). The $\Gamma_1 \rightarrow \Gamma_4$ gap practically does not depend on J . The reduced temperature dependence is a result of cancellation of temperature-dependent parts of the induced moments $\mu_B \langle \hat{l}_z \rangle$ and $\mu_B \langle 2\hat{s}_z \rangle$ that both deviate from a constant above 300 K due to increasing population of the excited-state triplet Γ_4 . See supplementary material for an illustration and for additional details of the J -dependence of χ_{imp} .

In summary, making use of the LDA+ED calculations with $U = 6.5$ eV and $J = 0.5$ eV we obtain a non-magnetic singlet ground state with $n_f \approx 4.5$ for Pu atoms in PuO₂. The LDA+ED yields an insulating electronic structure consistent with the experimental photoelectron spectra. The band gap is found to be 1.8 eV. The energy difference between the ground state and the first excited triplet state is 126 meV, in agreement with the experimental inelastic neutron scattering spectra. The calculated singlet ground state and the consequent non-magnetic behavior have a lot in common with the outcome of the crystal-field theory, the significant improvement is that LDA+ED achieves these features for a realistic non-integer occupation of the Pu f orbitals. We emphasize that we did not adjust the model parameters to fit the experimental findings. Instead, we investigated the dependence of physically observable quantities on the choice of these parameters.

The financial support from the Czech Republic Grant

GACR P204/10/0330 is acknowledged.

**Supplemental Material for
Non-magnetic ground state of PuO₂**

ANALYSIS OF THE LDA+U RESULTS

There are a number of recent papers reporting the LDA/GGA+U calculations for PuO₂ (see for instance Ref. [24] and references therein). They obtain an antiferromagnetic ground state, but often neglect spin-orbit coupling and use oversimplified treatment of the electron-electron Coulomb and exchange interactions. Nakamura *et al.* [7], and later Suzuki, Magnani and Oppeneer [8], have shown that constrained non-magnetic LDA+U calculations yield an insulating electronic structure for PuO₂. However, this non-magnetic solution is not the variationally determined minimum-energy state [6, 7]. The ferromagnetic and antiferromagnetic spin-polarized solutions are lower in energy and hence the non-magnetic insulating solution of Refs. [7, 8] is not the LDA+U ground state.

Below we perform an additional analysis of our own calculations using the conventional LDA+U. For the values of $U = 4$ eV and $J = 0$ eV our results are in agreement with those of Suzuki *et al.* [8], and show an insulating state with the band gap of 1.8 eV and the f -states occupation $n_f = 4.54$. The total density of states (TDOS), the O atom p -state and the Pu atom f -state partial DOS are shown in Fig. S1.

When a realistic non-zero $J = 0.5$ eV is included, and $U = 4.5$ eV is adopted (this choice keeps the effective $(U - J) = 4.0$ eV), the unoccupied part of the DOS changes substantially. The narrow empty f -peak shifts down in the energy, and the band gap is reduced to the value of 1.1 eV. For the realistic value of exchange J (Hund's exchange), the Coulomb $U = 6.5$ eV is needed to recover the band gap of 1.8 eV (see Tab. S1 and Fig. S1). Indeed, this non-magnetic LDA+U solution is not the true ground state for PuO₂, and allowing for the spin polarization will lower the total energy [7].

TABLE S1: Occupation n_f of the f shell and the band gap (eV) calculated in LDA+U as functions of the Coulomb U and the exchange J .

$[U, J]$ (eV)	[4.0, 0.0]	[4.5, 0.5]	[5.5, 0.5]	[6.5, 0.5]
n_f	4.54	4.56	4.52	4.48
E_g (eV)	1.8	1.1	1.3	1.8

THE ANDERSON IMPURITY MODEL

The Anderson impurity model including the spin-orbital coupling is block-diagonal in the occupation-number basis, with each block corresponding to a particular total number of electrons in the model N_{tot} . The blocks relevant for our problem correspond to N_{tot} equal 17, 18 (the ground state is in this block) and 19. The model is solved for these fillings with the aid of the Lanczos method using ARPACK [25] and an in-house code. Although this technique is efficient, the calculations still take a lot of time and require a large amount of RAM due to large dimensions of the blocks, namely 21.4, 13.1 and 6.9 million. In order to make the problem more manageable, we reduce the many-body basis using the method of Gunnarsson and Schönhammer [26] that is related to the expansion in the hopping integrals V_k around the atomic limit. For instance, the reduced Fock space containing all contributions up to the second order of this expansion reads as $\{|f^n\rangle, |f^{n+1}\underline{b}\rangle, |f^{n+1}\underline{bb}\rangle\}$ where \underline{b} indicates a hole in the bath orbitals. The size of the basis can thus be specified by the maximum number of bath holes present, N_h .

Since the hybridization parameters $V_k \approx 1.5$ eV are not particularly small, it is not obvious if the expansion converges quickly enough to be actually useful. Explicit convergence analysis nevertheless shows that $N_h = 3$ gives essentially converged f -electron spectrum and magnetic susceptibility, whereas $N_h = 2$ is still too small. The spectral density calculated as $N(\epsilon) = -\text{Im Tr}[G_{\text{imp}}(\epsilon + i\delta)]/\pi$ is shown in Fig. S2A. There is an approximately 1 eV shift of the spectrum to the right and the gap is about 0.5 eV smaller when the basis is increased from $N_h = 2$ to $N_h = 3$. No substantial changes in the spectrum are found with the further increase of N_h .

The spectral density for $N_h = 2$ closely resembles the f -DOS from Fig. 3 of Ref. [17] that employs the so-called one-crossing approximation which is also a variant of the expansion around the atomic limit. The total density of states (TDOS), the Pu atom f -state, and the O atom p -state partial DOS are shown in Fig. S2B for $N_h = 2$. There are some differences with the DOS for $N_h = 3$ shown in Fig. 2 of the main text. The band gap becomes slightly larger, ≈ 2 eV, for $N_h = 2$. The occupied part of the Pu- f -DOS is shifted to the left by about 0.5 eV, and the O- p -states are following this shift. This is due to the shift of the SDOS shown in Fig. S2A. There are no noticeable changes at the bottom of the valence band where the O- p -states dominate.

ADDITIONAL DETAILS FOR EQS. (2) AND (3)

The detailed description of the charge self-consistency procedure is given in Ref. [13]. In brief, once the occupation matrix $n_{\gamma_1\gamma_2}$ is evaluated from the solution of

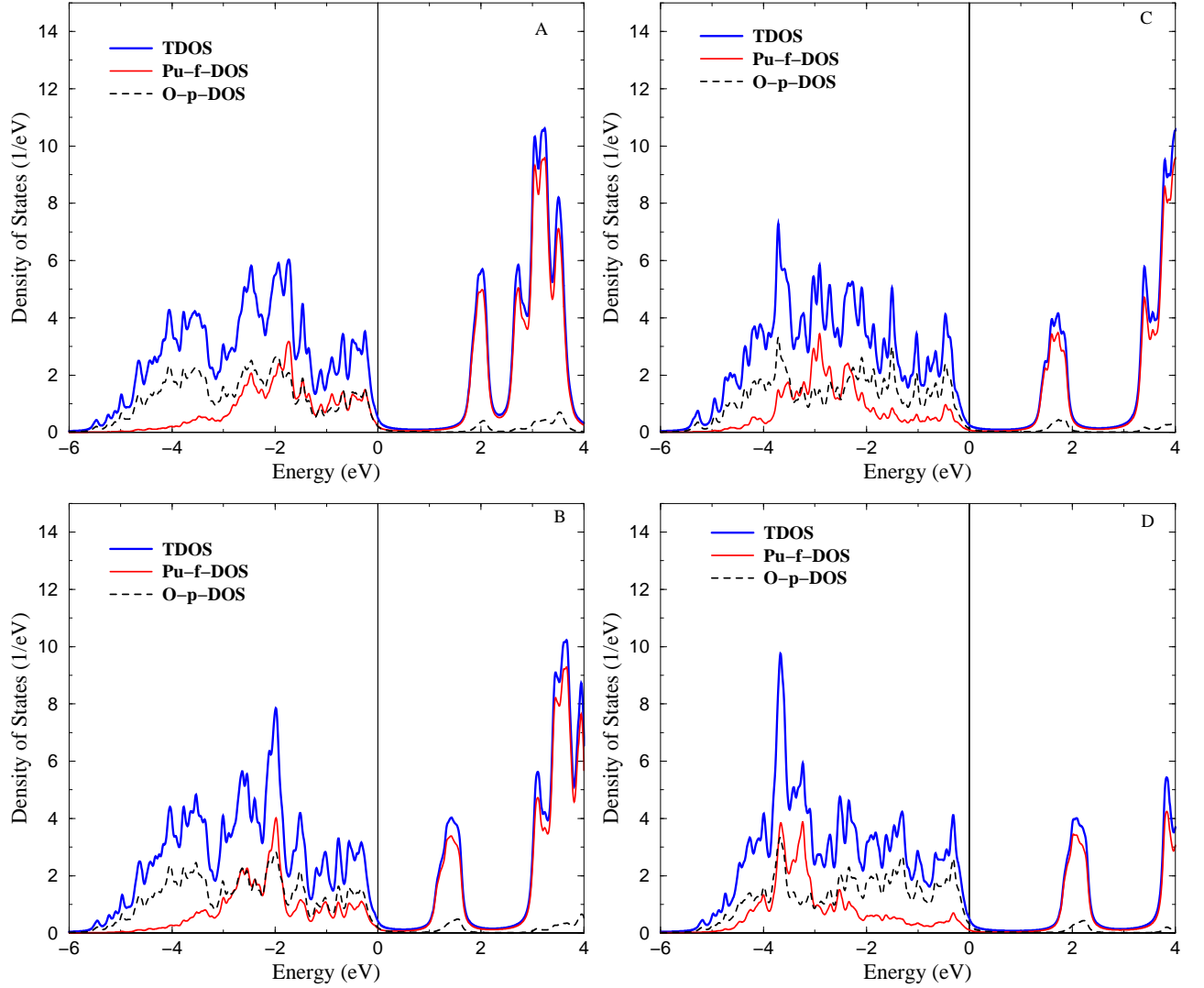


FIG. S1: (Color online) The total, O-*p* and Pu-*f*-projected DOS from LDA+U calculations with $U = 4$ eV, $J = 0$ eV (A), and $U = 4.5$ (B), 5.5 (C), 6.5 (D) eV, and $J = 0.5$ eV .

TABLE S2: Occupation n_f of the *f* shell, and the band gap (eV) calculated in LDA+ED as a function of the Coulomb U , and the exchange J .

$[U, J]$ (eV)	[4.5, 0.5]	[5.5, 0.5]	[6.5, 0.5]
n_f	4.58	4.55	4.52
E_g (eV)	-	1.4	1.8

Eq. (1), it is used to construct the effective ‘‘LDA+U potential’’, $V_U = \sum_{\gamma_1 \gamma_2} |\phi_{\gamma_1}\rangle V_U^{\gamma_1 \gamma_2} \langle \phi_{\gamma_2}|$, where

$$V_U^{\gamma_1 \gamma_2} = \sum_{\gamma \gamma'} \left(\langle \gamma_2 \gamma | V^{ee} | \gamma_1 \gamma' \rangle - \langle \gamma_2 \gamma | V^{ee} | \gamma' \gamma_1 \rangle \right) n_{\gamma \gamma'} - V_{dc} \delta_{\gamma_1 \gamma_2}. \quad (\text{S1})$$

Up to now, our considerations did not depend on the choice of the basis set. The method becomes basis-set

dependent when a projector of the Bloch-state solutions of Eq. (2) on the local basis $\{\phi_\gamma\}$ is specified. The FP-LAPW method uses a basis set of plane waves that are matched onto a linear combination of all radial solutions (and their energy derivative) inside a sphere centered on each atom. In this case, we make use of the projector technique which is described in detail in Ref. [18]. It is important to mention that, due to the full-potential character of the method, care should be taken to exclude the double-counting of the *f*-states non-spherical contributions to the LDA and LDA+U parts of potential in Eq. (2).

The selfenergy Σ entering Eq. (3) is obtained as

$$\Sigma = \hat{G}_{\text{imp}}^{-1} [\hat{H}_{\text{imp}}^{(0)}] - \hat{G}_{\text{imp}}^{-1} [\hat{H}_{\text{imp}}], \quad (\text{S2})$$

where $\hat{G}_{\text{imp}}[\hat{H}_{\text{imp}}]$ represents the Green’s function matrix in the *f*-orbital subspace evaluated for a general impurity

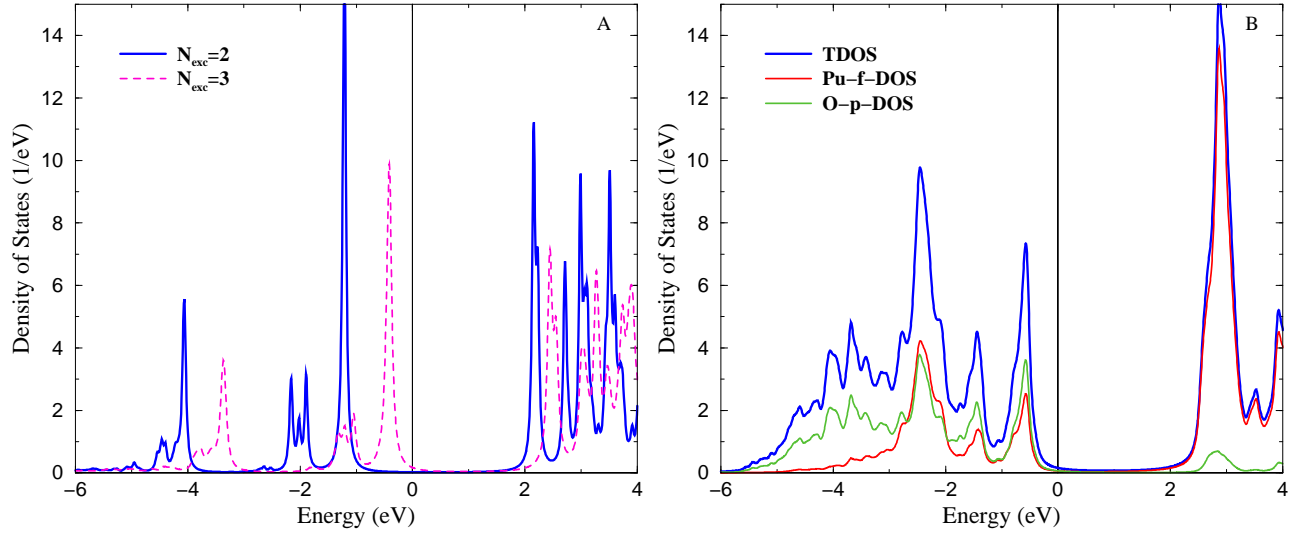


FIG. S2: (Color online) The spectral f -DOS calculated in the impurity model for $U = 6.5$ eV, $J = 0.5$ eV evaluated for different sizes of the many-body basis (A). The total, O- p and Pu- f -projected DOS from LDA+ED calculations with $N_h = 2$ (B).

Hamiltonian defined in Eq. (1). The matrix $\hat{G}_{\text{imp}}[\hat{H}_{\text{imp}}^{(0)}]$ is the Green's function of the same Hamiltonian without the Coulomb interaction (fifth term).

MAGNETIC SUSCEPTIBILITY IN THE IMPURITY MODEL

It is indicated in the main text that the magnetic susceptibility is a decreasing function of the Hund's exchange J . Figure S3 illustrates this dependence in detail for the crystal-field theory (χ_{CF}) as well as for the impurity model with hybridization (χ_{imp}). In principle it is possible to reduce the susceptibility down to the experimental value if J is raised to 1.0 eV but such J seems unrealistically high since it is about 20% larger than the atomic Hartree-Fock value [16].

The suppressed temperature dependence is a result of cancellation of temperature dependent parts of the induced moments $\mu_B \langle \hat{l}_z \rangle$ and $\mu_B \langle 2\hat{s}_z \rangle$ that both deviate from a constant above 300 K due to increasing population of the excited-state triplet Γ_4 . Figure S4 illustrates this cancellation: the susceptibility is split into two parts, $\chi_{\text{imp}} = \chi_l + \chi_s$, where χ_l measures the response of the orbital moment, $\chi_l(T) = \mu_0 N_A \mu_B \langle \hat{l}_z \rangle / B_z$, and χ_s measures the response of the spin moment, $\chi_s(T) = \mu_0 N_A \mu_B \langle 2\hat{s}_z \rangle / B_z$.

The effect of hybridization with ligand states can be approximately represented in the crystal-field theory by means of the so-called orbital reduction factor k that enters the Zeeman term in the hamiltonian

$$\hat{H}_Z^f = - \sum_{m\sigma} \mu_B B_z [k\hat{l}_z + 2\hat{s}_z]_{mm}^{\sigma\sigma} \hat{f}_{m\sigma}^\dagger \hat{f}_{m\sigma}$$

and also the magnetic moment induced in the f shell

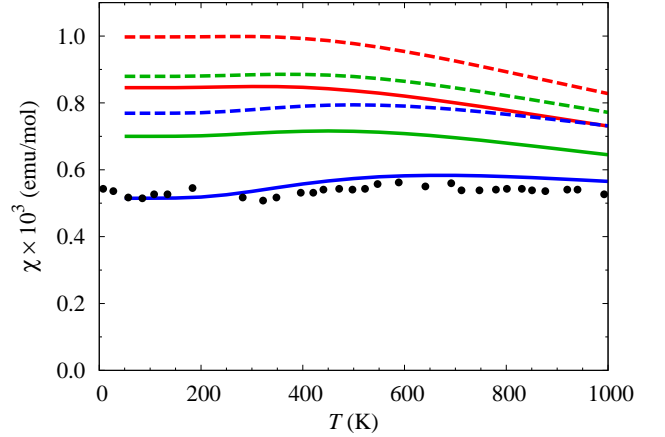


FIG. S3: (Color online) Magnetic susceptibility as a function of the Hund's exchange; $J = 0.5$ eV (red), 0.65 eV (green) and 1.0 eV (blue). We compare χ_{imp} from the impurity model (solid lines) with χ_{CF} from the crystal-field theory (dashed lines). Experimental data [2] are shown as black dots.

$m_z = \mu_B \langle k\hat{l}_z + 2\hat{s}_z \rangle$. The susceptibilities χ_{imp} shown in Fig. S3 can be recovered in the crystal-field theory by setting k to 0.965 for $J = 0.5$ eV, 0.955 for $J = 0.65$ eV, and 0.932 for $J = 1.0$ eV. The experimental data would correspond to $k = 0.905$ for $J = 0.65$ eV as shown in [5].

-
- [1] C. E. McNeilly, J. Nucl. Mater. **11**, 53 (1964).
 - [2] G. Raphael and R. Lallemand, Solid State Commun. **6**, 383 (1968).
 - [3] H. Yasuoka *et al.*, Science **336**, 901 (2012).
 - [4] P. Santini *et al.*, Rev. Mod. Phys. **81**, 807 (2009).

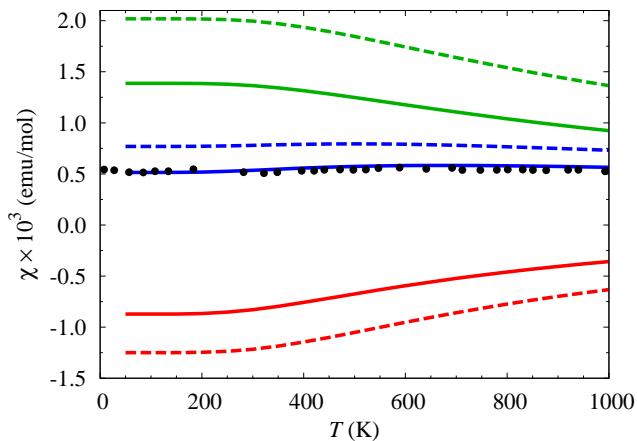


FIG. S4: (Color online) Cancellation of the temperature dependence in the total magnetic susceptibility (blue) for $J = 1.0$ eV. The orbital part χ_l is shown in green, the spin part χ_s in red. Solid lines correspond to χ_{imp} , dashed lines to χ_{CF} .

- [5] S. Kern and *et al.*, Phys. Rev. B **59**, 104 (1999).
 [6] X.-D. Wen *et al.*, Chemical Review **113**, 1063 (2013).
 [7] H. Nakamura, M. Machida, and M. Kato, Phys. Rev. B **82**, 155131 (2010).
 [8] M.-T. Suzuki, N. Magnani, and P. M. Oppeneer, Phys. Rev. B **88**, 195146 (2013).
 [9] J. Kolorenc, A. Poteryaev, and A. I. Lichtenstein, Phys. Rev. B **85**, 235136 (2012).
 [10] A. B. Shick, J. Kolorenc, J. Ruzs, P. M. Oppeneer, A. I. Lichtenstein, M. I. Katsnelson, and R. Caciuffo, Phys. Rev. B **87**, 020505 (2013).
 [11] A. I. Lichtenstein and M. I. Katsnelson, Phys. Rev. B **57**, 6884 (1998).
 [12] A. Hewson, *The Kondo Problem to Heavy Fermions* (Cambridge University Press, 1993).
 [13] A. B. Shick, J. Kolorenc, A. I. Lichtenstein, and L. Havela, Phys. Rev. B **80**, 085106 (2009).
 [14] N. Magnani, P. Santini, G. Amoretti, and R. Caciuffo, Phys. Rev. B **71**, 054405 (2005).
 [15] P. Novak, K. Knizek, and J. Kunes, Phys. Rev. B **87**, 205139 (2013).
 [16] K. Moore and G. van der Laan, Rev. Mod. Phys. **81**, 235 (2009).
 [17] Q. Yin, A. Kutepov, K. Haule, G. Kotliar, S. Y. Savrasov, and W. E. Pickett, Phys. Rev. B **84**, 195111 (2011).
 [18] A. B. Shick, A. I. Lichtenstein, and W. E. Pickett, Phys. Rev. B **60**, 10763 (1999).
 [19] A. B. Shick and W. Pickett, Phys. Rev. Lett. **86**, 300 (2001).
 [20] A. Kotani and T. Yamazaki, Prog. Theor. Phys. Suppl. **108**, 117 (1992).
 [21] M. Butterfield and *et. al.*, Surface Sci. **74**, 571 (2004).
 [22] T. Gouder, A. Seibert, L. Havela, and J. Rebizant, Surface Sci. **601**, L77 (2007).
 [23] T. Gouder, A. Shick, and F. Huber, Topics in Catalysis **56**, 1112 (2013).
 [24] G. Jomard, B. Amadon, F. Bottin, and T. M., Phys. Rev. B **78**, 075125 (2008).
 [25] R. B. Lehoucq, D. C. Sorensen, and C. Yang, *ARPACK Users' Guide: Solution of Large-Scale Eigenvalue Problems with Implicitly Restarted Arnoldi Methods* (Society for Industrial and Applied Mathematics, Philadelphia, 1998).
 [26] O. Gunnarsson and K. Schönhammer, Phys. Rev. B **28**, 4315 (1983).